



Temporal and spatial changes in grain size on a macro-tidal channel-flat complex: results from Kingsport, Nova Scotia, Bay of Fundy

Brent A. Law^{1,2} · Paul S. Hill² · Timmothy G. Milligan¹ · Vanessa Zions¹

Received: 2 May 2018 / Accepted: 12 November 2018 / Published online: 23 November 2018
© Crown 2018

Abstract

Understanding the processes that lead to seasonal changes in grain size on muddy macro-tidal flat and channel complexes will assist efforts to predict future changes caused by climate change and construction of infrastructure like tidal power generators, wind farms, and causeways. Surficial sediment samples were collected for disaggregated inorganic grain size (DIGS) analysis every month for 1 year from a tidal flat and from a tidal channel and its banks in Kingsport, NS, Canada, which is located in the Minas Basin of the Bay of Fundy. A process-based parameterization of the DIGS distribution was used to determine floc fraction, representative of the percentage of fine-grained material deposited to the seabed in flocs. Small changes in floc fraction occurred seasonally in the channel. Values were higher in late winter and lower in late summer. A more pronounced seasonal variation in floc fraction was observed on the tidal flats. Observed changes in floc fraction correlated with elevation. Results from this study are discussed in terms of the controls on floc fraction which include suspended particulate matter concentration (SPM), turbulence, and stickiness in the water column, all of which can be used to understand the formative processes responsible for shaping the bottom sediment texture.

Keywords Grain size · Macro-tidal · Flocs · Floc fraction · Tidal flats

1 Introduction

Tidal flats provide important habitat for shore birds, benthic invertebrates, and commercial fish species but unfortunately also act as repositories for contaminants (e.g., Widdows and Brinsley 2002). Intertidal deposits provide natural coastal defenses that will respond in poorly understood ways to future rises in sea level (e.g., Reed et al. 1999; Widdows and Brinsley 2002; Townend and Whitehead 2003; Kirwan et al. 2010) and to installations of infrastructure such as tidal power generators, wind farms, and causeways (van Proosdij et al.

2009; Wu et al. 2011; Ashall et al. 2016). The wide variety of functions of intertidal deposits has motivated substantial research into not only their morphology but also into the processes that control their morphology.

Knowledge of sediment transport is vital to understanding intertidal deposits. The processes driving sediment erosion, deposition, and transport in these environments are numerous, complicated, and inter-related (Eisma 1998). Water motions are induced by tides, wind-driven currents, waves, density contrasts, and drainage from flats (Le Hir et al. 2000). Biophysical interactions are important, with sediment affecting the biota and the biota affecting sedimentary processes (e.g., Austen et al. 1999; Black et al. 2002; Widdows and Brinsley 2002; Garwood et al. 2015). Sediments in intertidal deposits are characteristically heterogeneous, with marked variability in sediment size and composition (Eisma 1998; Holland and Elmore 2008).

Grain size is a fundamental defining property of soft-sediment benthic ecosystems. Grain size distributions hold within them a record of the processes responsible for the formation of sedimentary deposits (Kranck 1973, Kranck 1975, Kranck and Milligan 1985). Grain-size analysis is especially useful for description of tidal flats because flats are generally composed of mixed grain-sized beds. Tidal flats often have

This article is part of the Topical Collection on the *14th International Conference on Cohesive Sediment Transport in Montevideo, Uruguay 13-17 November 2017*

Responsible Editor: Carl Friedrichs

✉ Brent A. Law
lawb@mar.dfo-mpo.gc.ca

¹ Fisheries and Oceans Canada, Bedford Institute of Oceanography, Dartmouth, NS B2Y 4A2, Canada

² Department of Oceanography, Dalhousie University, Halifax, NS B3H 4R2, Canada

abrupt transitions from sands at lower elevations where tidal stresses are larger to fine muds at higher elevations, where shear stresses are lower. The processes of deposition, erosion, and transport of sand sized grains are relatively well understood (Soulsby 1997). Early results of Shields (1936) showed that sand transport is a function of grain size and the shear stress imposed at the seabed, with larger grains progressively eroded as shear stress increases. Mud, or the < 63- μm fraction, behaves in a different manner. Particle-particle electro-chemical and organic bonding acting on the large surface areas of small particles makes mud cohesive (Hill et al. 2001; van Ledden et al. 2004; Milligan et al. 2007). Cohesion of muds increases the erosion resistance, so the transport of mud particles can require the same or greater shear stresses as are required to move much larger sand size grains (Wiberg and Smith 1987; Wiberg et al. 1994).

The mud fraction within surficial sediments is important for many reasons. Mud often has high water content, which reduces their ability to support the weight of humans or vehicles (Rose and Willig 2004; Harris et al. 2008). Increasing mud content on the seabed can increase the primary productivity by microphytobenthos, which can result in changes to the food chain (Ysebaert and Herman 2002). Changes in grain size can result in changes to channel stability and other morphodynamic features (Dyer et al. 2000). Finally, the mud fraction, and more specifically the < 16- μm fraction, plays a large role in the trapping and the sequestering of surface reactive pollutants such as heavy metals, PCB's, PAH's, and other persistent organics (Zwolsman et al. 1996; Milligan and Loring 1997; Santschi et al. 1997).

The deposition, transport, and erosion of fine sediment are affected fundamentally by flocculation (McCave 1984; Kranck and Milligan 1991). Flocculation is the process whereby particles clump, either by electrochemical attraction or organic bonding, to form “flocs.” Flocs sink much faster than the component particles within them (Sternberg et al. 1999). Therefore, settling within flocs is responsible for the majority of deposition of fine-cohesive sediments (Kranck 1980; McCave et al. 1995; Curran et al. 2002).

A promising tool for understanding fine-grained cohesive sediment behavior is a process-based analysis of disaggregated inorganic grain size (DIGS) distributions (Kranck and Milligan 1991; Kranck et al. 1996a, 1996b; Curran et al. 2004). A DIGS sample is one in which all organics have been removed, and the bonds between the remaining inorganic component grains have been disrupted. DIGS distributions can be used to infer how much of a deposit was delivered to the seabed as flocs versus single grains, thereby providing a parametric description that accounts for the dominant depositional processes. This process-based interpretation of a DIGS sample relies on the assumptions that material in suspension is composed either of flocs or of single grains and that flocs incorporate into their structure all suspended sediment sizes

in an unbiased way (Kranck et al. 1996a; Curran et al. 2004). Deposition of flocs does not alter the overall size distribution of the remaining suspended population. Single-grain settling, however, sorts particles according to size, thereby producing evolution in the size distribution of the remaining population (Kranck et al. 1996a, 1996b).

The process-based parameterization of DIGS can be used to quantify the spatial and temporal changes in flocculation in the overlying water column that were responsible for the changes in the texture of fine-grained bottom sediments (Christiansen et al. 2000; Curran et al. 2004; Fox et al. 2004; Milligan and Law 2005; George et al. 2007; Milligan et al. 2007; Law et al. 2013; O’Laughlin et al. 2014). Christiansen et al. (2000) focused on intertidal sediment and showed that the fraction of sediment deposited as flocs, which is termed the “floc fraction,” decreased along a transect extending from the edges of a secondary channel into the interior of a vegetated mesotidal salt marsh. O’Laughlin et al. (2014) studied a hyper-tidal creek in the Bay of Fundy and showed that the suspension in that creek was consistently and highly flocculated and that the large incoming suspended sediment concentration (> 100 mg/L) caused extensive flocculation and rapid settling as hydrodynamic forces waned. On a mesotidal mudflat in Willapa Bay, Washington, Law et al. (2013) showed that floc fractions in the seabed were related to elevation on the flat. Larger floc fractions were found in tidal channels and on channel banks, and smaller floc fractions were found higher on the flats.

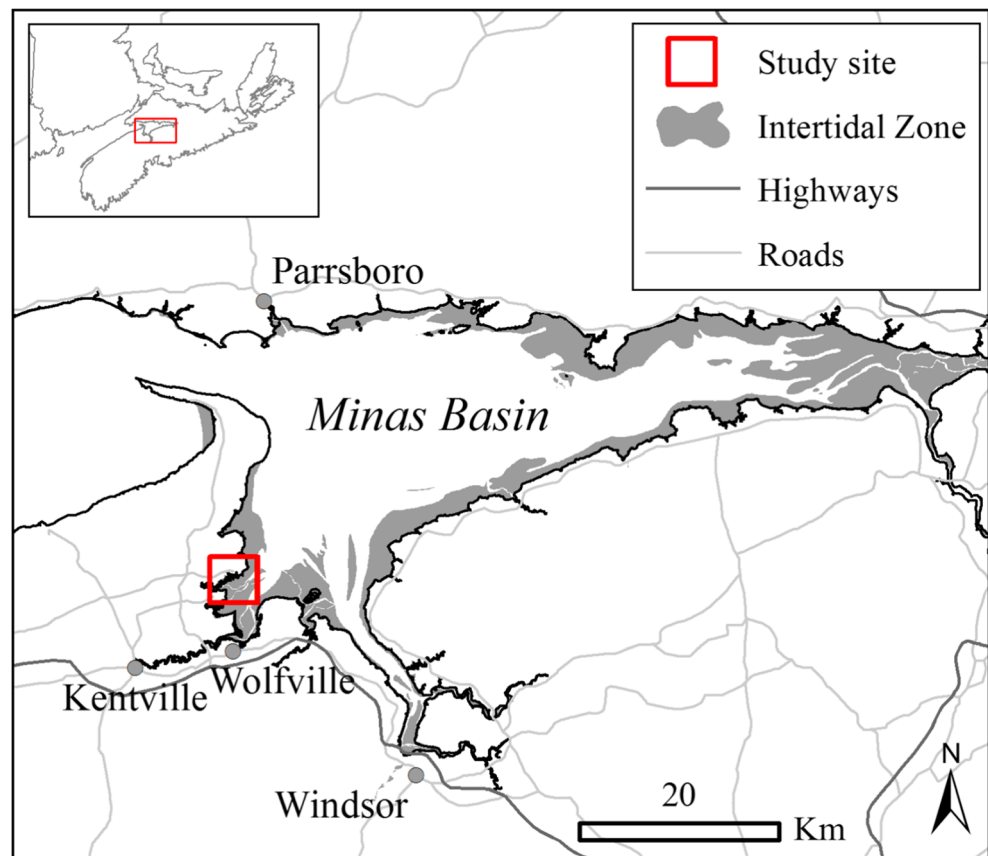
The goal of this present paper is to apply the process-based parameterization of DIGS to understanding of the role of flocculation in determining the spatial and temporal variations of grain size on a muddy, macro-tidal flat. Understanding the natural variation of sediment in suspension and on the seabed (i.e., baseline conditions) in the Upper Bay of Fundy is essential for the development of coupled hydrodynamic-sediment transport models. Operational models can then be used to predict the hydrodynamics and sediment dynamics in the creeks, on tidal flats, and in other areas, which in turn can be used to explore the effects on sedimentation caused by anthropogenic activity.

2 Methods

2.1 Overview

The study site was the Kingsport, Nova Scotia, tidal-flat complex, in the Minas Basin, which is part of the inner Bay of Fundy (Fig. 1). The site experiences mixed, slightly asymmetric semi-diurnal tides with mean tidal range of approximately 11.5 m and with maximal current velocities at mid-flood tide (Amos et al. 1988, 1992; Faas et al. 1993; Garwood et al. 2015). Although the area experiences limited wave activity,

Fig. 1 Map of Minas Basin and our study site at Kingsport as indicated by the thick red box



due to its sheltered location, wind-waves can be responsible for significant sediment resuspension, especially during winter (Ashall et al. 2016). Amos and Mosher (1984) classified the area as composed of mostly glaciated sediments rich in illite and chlorite and reduced in smectite and kaolinite, which leads to particle adhesion controlled by biological activity and organic glue and not cohesion by particle-particle bonding. Biological activity increases during the summer months, driven by an increase in diatom mats and foraging by *Corophium volutator* and shore birds (Daborn 1991; Garwood et al. 2015). In the winter months, ice rafting and anchor-ice formation can also play roles in sediment transport processes (Knight and Dalrymple 1976; Gordon and Desplanques 1983).

From April 2012 to March 2013, around the 20th day of each month, a series of 60 stations, 37 from the tidal flat and 23 from the tidal channel (Fig. 2), were sampled for bottom sediment disaggregated inorganic grain size (DIGS) analysis. Samples were collected on foot during low water using a spoonula to sample only the top 0.5 cm of the bottom sediment. Sampling was conducted between 3 and 4 h after high tide.

2.2 LiDAR data

LiDAR data were collected at low, low-tide conditions in an east to west and then overlapping north to south direction by

Fugro, Inc., for the Canadian Hydrographic Service (CHS) of the Department of Fisheries and Oceans, Canada. Vertical datum is referenced to Canadian Geographic Vertical Datum of 1928 (i.e., CGVD) and horizontal datum to North American Datum of 1983 (i.e., NAD83). Independent ground control points in the vertical (z) and horizontal (x - y) were acquired using static positioning techniques throughout the project area. The processed LiDAR data were compared to three ground control points within the project area. A triangulated irregular network (TIN) model was created, and a z value was interpolated. A regional, LiDAR generated digital-elevation-model, DEM, was developed with error in the horizontal < 1.0 m and error in the vertical < 0.05 m (Fig. 2). Data points collected during the monthly regional grain-size surveys were plotted in the GIS software program ARC GIS (ESRI ©) and placed onto the LiDAR composite image (Fig. 2). The horizontal uncertainty of the handheld GPS, Garmin 76CS, used to obtain the data locations of the monthly sampling was 3–4 m.

2.3 Grain-size analysis

The disaggregated inorganic grain size (DIGS) distributions of bottom sediment samples were determined using a Coulter Multisizer III. Organic matter was removed from bottom sediments with 35% hydrogen peroxide (H_2O_2). Prior to analysis

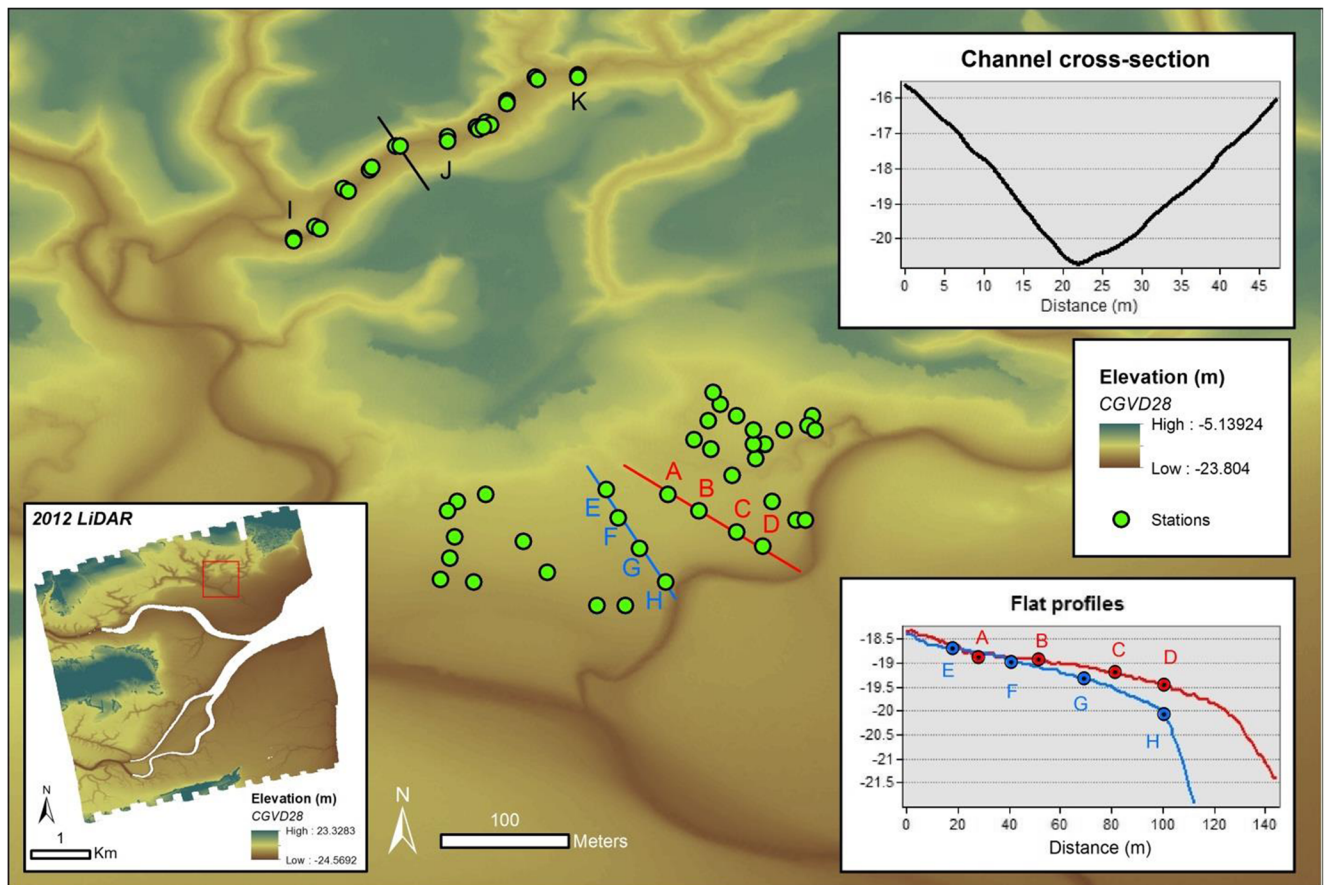


Fig. 2 LIDAR and sample station data from the Kingsport tidal-flat complex. Elevation in meters is referenced to CGVD28, while horizontal points are referenced to NAD-83. Inserts from top right to bottom left include cross-section profile of the channel in distance vs.

elevation in meters and is marked by the black line near station J, flat profiles from upper to lower flat and are marked by the red and blue line and are distance vs. elevation in meters and the full 2012 LIDAR survey of the area

on the Multisizer, inorganic sediments were resuspended in a 1% NaCl solution and then disaggregated with a sapphire-tipped ultrasonic probe. Three tubes, with apertures of 30, 200, and 400 μm, were used to obtain the DIGS distribution over a size range from 0.8 to 240 μm. Particle sizes were binned in a 1/5 phi interval (i.e., $\phi (\Phi) = -\log_2 D$; D = diameter in mm). The DIGS obtained from the Multisizer are expressed as log of equivalent volume fraction versus log of the diameter. Volume fraction is assumed to equal mass fraction, which implies constant particle density across all sizes. Error in the size measurements of the Coulter Multisizer III is < 10%. For a complete description of the methods of the particle size analysis, see Kranck and Milligan (1979) and Milligan and Kranck (1991).

DIGS distributions were analyzed using standard granulometric parameters and the inverse model of Curran et al. (2004). The inverse model determines the relative proportions of the bottom sediment delivered to the seabed as flocs or single grains. Median diameter, d_{50} , and other grain-size descriptors such as d_{75} (the grain size between the third and fourth quartiles of the population), d_{95} , d_{84} , d_{25} , d_{16} , and d_5 were calculated. Values for d_{50} and other

granulometric parameters are expressed in micrometers. These values were converted to phi units (by formula above) and a method-of-moments analysis was completed for each grain size distribution to determine the geometric mean diameter (GMD), inclusive graphic standard deviation (θ_1), inclusive graphic skewness (SK_1), and graphic Kurtosis or peakedness (K_G), following Folk and Ward (1957).

The inverse floc model of Curran et al. (2004) applies a non-linear least squares fit to the DIGS curves, taking the form of the equation:

$$J(i) = \beta \left(\frac{d_i}{d_o} \right)^m e^{-\left(\frac{d_i}{d_a} \right)^2} \left(1 + \left(\frac{d_i}{d_f} \right)^2 \right) \quad (1)$$

where $J(i)$ is the mass flux of size class i to the seabed in $\text{kg m}^{-2} \text{s}^{-1}$, β equals the flux to the seabed ($\text{kg m}^{-2} \text{s}^{-1}$) of a reference grain-size diameter (d_o) (m) contained within flocs, and d_i is the diameter of size class i (m). Source slope, m (dimensionless), reflects the relative proportions of coarse and fine material found in the bottom sediment and is a function of how the parent rock weathers (Kranck et al. 1996a).

The parameter \hat{d} (m) is the grain size whose concentration has fallen to $1/e$ of its initial concentration in the parent population and is used as an approximation for the largest grain size in suspension. Floc limit, d_f (m), is the grain diameter for which the fluxes of mass to the seabed from flocs and single grains are equal. Mathematically, the floc limit is defined as:

$$d_f = \sqrt{\frac{18w_f f \mu}{(1-f)(\rho_s - \rho)g}} \tag{2}$$

where w_f is the settling velocity of flocs (m s^{-1}), f (dimensionless) is the mass fraction of material bound within flocs in suspension, μ is the dynamic viscosity ($\text{kg m}^{-1} \text{s}^{-1}$), ρ_s is the sediment density (kg m^{-3}), ρ represents the fluid density (kg m^{-3}), and g is the gravitational acceleration (m s^{-2}). Finally, floc fraction, K_f (dimensionless), is the mass fraction of material that was deposited to the seabed in flocs. It is described by the equation

$$K_f = \frac{\sum_{i=1}^{n_{class}} C(i)}{\sum_{i=1}^{n_{class}} \left(1 + \left(\frac{d_i}{d_f}\right)^2\right) C(i)} \tag{3}$$

where $C(i)$ is the concentration of size class i (kg m^{-3}), and n_{class} represents the number of size classes present in the DIGS distribution. Sensitivity analysis of the inverse model revealed that random noise of up to 20% introduced to the DIGS curves did not significantly affect the estimated parameters of m , \hat{d} , d_f , and K_f (Curran et al. 2004). Error introduced to fitting the model to the DIGS distributions is assumed to be less than that introduced from error in Coulter Counter measurements (i.e., < 10%) and therefore is unlikely to produce spurious trends in the estimated parameters. This study focuses on floc fraction and how it varied as a function of position on the flats and as a function of time.

2.4 Physical oceanography/wave data

An upward-looking Acoustic Doppler Current Profiler, ADCP (2 MHz, Nortek Aquadopp), was deployed on a bottom-mounted frame in the middle of the tidal flat. The Aquadopp was deployed approaching spring tide for two tidal cycles in January 2013 and for 4.5 tidal cycles approaching neap tide in June 2103. The ADCP was positioned 0.10 m above the seabed in a weighted aluminum channel. Data were collected in burst mode at 8 Hz and 2400 samples. This frequency of sampling allowed data collection for 5 min every 15 min and enabled the measurement of both current velocities and orbital velocities due to waves. A wave-current-interaction model developed by Grant and Madsen was used

to determine the combined wave-current shear stress at the seabed (Grant and Madsen 1986; Madsen 1994).

3 Results

The bed surface sediments from the Kingsport tidal-flat complex were composed mainly of mud with geometric mean diameters < 63 μm and ranged from 12.3 to 43.6 μm over the study period, with an average of 23.6 μm . The < 16- μm fraction was variable and ranged from 22.1 to 73.9% based on the 707 samples analyzed with an average < 16- μm fraction of 49.4%. The mud fraction (< 63 μm) in samples analyzed ranged from 85.5 to 100% with an average of 96.1%. Of the 707 samples analyzed, < 5% had a mud fraction that was < 90%.

The average grain size of samples collected in the tidal channel at Kingsport over the course of the 12-month study period had slightly higher values of d_{50} in winter and lower in summer (Fig. 3). Average median grain diameter, d_{50} , ranged from a low of 14.4 μm in April to a high of 22.8 μm in October, but generally, d_{50} values ranged from 14 to 18 μm (Fig. 3; Table 1). The mud fraction from the samples collected in the channel ranged from 94.0 to 98.9% with the lowest and highest values coming from the summer and late winter/early spring, respectively (Table 1). Modal size ranged from 21.1 to 42.0 μm , with the range generally between 28 and 32 μm over the course of the 12-month study (Table 1).

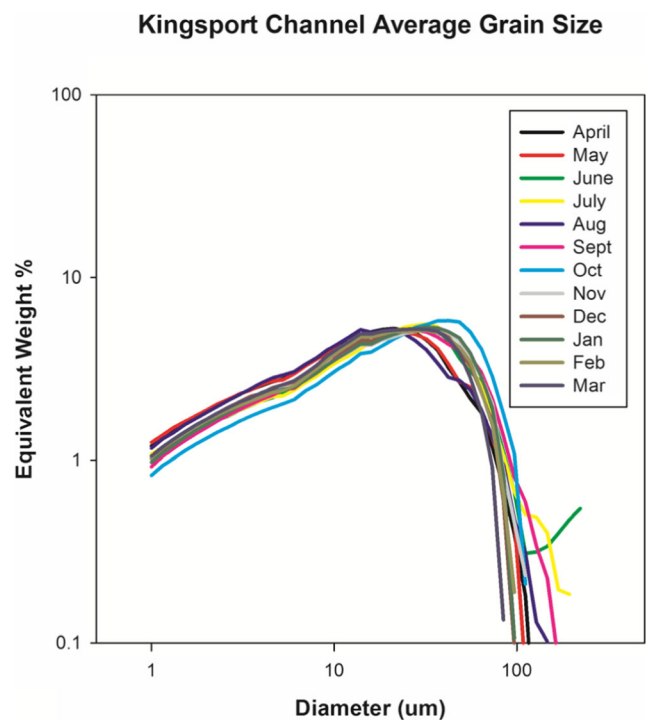


Fig. 3 Average DIGS from the Channel over the monthly sampling was expressed as equivalent weight percent versus diameter in micrometers. Size distributions do not vary markedly among months

The along-channel grain size showed a slight coarsening moving from the channel mouth at the seaward station I to the landward station K (Figs. 2 and 4). Two samples from stations I, J, and K in the channel were averaged over the 12-month study period ($N = 24$ from each station) and examined. Median grain diameter, d_{50} , ranged from $18.3 \mu\text{m}$ at the seaward station I to $16.8 \mu\text{m}$ near the middle of the channel section at station J to $16.4 \mu\text{m}$ at the landward end of sample, called station K (Fig. 4; Table 2). The sand fraction remained relatively constant near 3% with slightly more sand in the bottom sediment at the seaward station I at 4.1% compared to closer to 3% at the inner stations, J and K (Table 2). Modal size from the three stations gave the best indication of a seaward coarsening of grain size with values ranging from $27.8 \mu\text{m}$ at station K to $36.8 \mu\text{m}$ at station I (Table 2).

Average grain size values from the Kingsport flat were more variable than the channel samples (Fig. 5). Median grain size values of flat samples ranged from 13.7 to $27.7 \mu\text{m}$. Generally, the higher d_{50} values, i.e., those $> 20 \mu\text{m}$, occurred in the later summer, fall, and early winter, and those with d_{50} values $< 20 \mu\text{m}$ usually occurred from late winter into spring (Table 3). The sand fraction of samples from the flat ranged from 1.7 to 6.8% with the larger fraction of sand generally found in the bed sediments at the same time as the higher d_{50} values. Modal size ranged from approximately $18 \mu\text{m}$ to $42 \mu\text{m}$, with values generally between 28 and $37 \mu\text{m}$, with the lowest values in the spring months between April and June (Table 3). The other main difference between the channel and flat samples was greater variability in the $< 16\text{-}\mu\text{m}$ fraction which ranged from 38.5 to 59.6% over the study period (Fig. 5; Table 3).

Inclusive graphic standard deviation, σ_1 , a measure of sorting, ranged from 1.16ϕ to 1.85ϕ , with an average of 1.56ϕ . These values indicate that the samples were poorly sorted (Folk 1968). Inclusive graphic skewness, a measure of the degree of asymmetry in the samples, ranged from 0.02 to

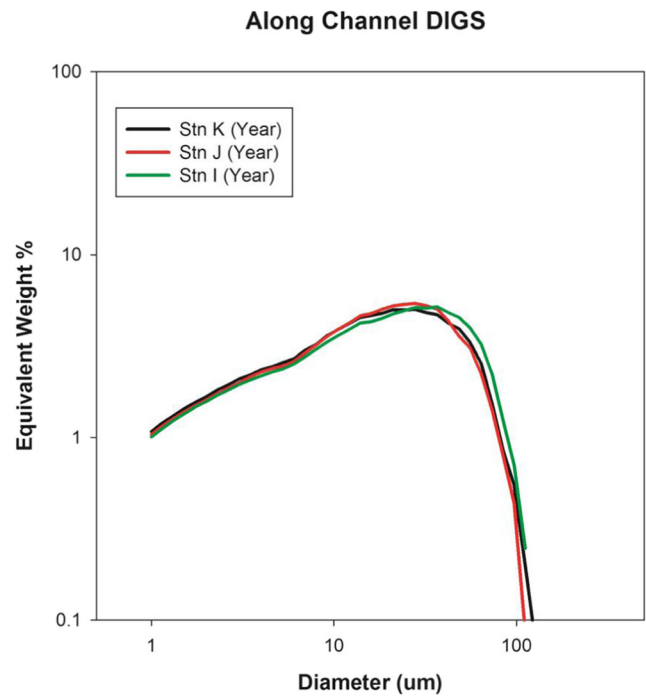


Fig. 4 Average DIGS from along the channel over the monthly sampling expressed as equivalent weight percent versus diameter in micrometers. Channel position does not have a large effect on grain size

0.51, with an average of 0.23, indicating that the samples were fine skewed (i.e., 0.1 to 0.3) (Folk 1968). Approximately 20% of the samples had skewness values between 0.3 and 0.5 and were classified as strongly fine skewed. Kurtosis, a measure of peakedness, ranged from 0.84 to 1.23, with an average value of 0.97. These values indicate that the distributions were platykurtic (i.e., between 0.9 and 1.11) (Folk 1968). When examining flat versus channel differences, samples collected from the flat had standard deviation values ranging from 1.46ϕ to 1.67ϕ with an average of 1.58ϕ (Table 4). Skewness values from flat samples ranged from 0.15 to 0.33 with an average of 0.25, and kurtosis values ranged from 0.93 to

Table 1 Yearly average grain size parameters from the tidal channel

Date	FF	< 4	< 16	< 63	d_{50}	d_{75}	d_{25}	d_5	d_{95}	d_{84}	d_{16}	Modal
Apr 12	0.75	20.5	58.4	97.5	14.4	28.2	5.9	1.8	66.1	37.3	3.7	21.1
May 12	0.57	20.9	58.0	97.2	14.4	29.0	5.8	1.8	67.6	38.4	3.7	21.1
Jun 12	0.50	17.1	49.0	94.0	18.7	36.2	7.5	2.0	91.6	47.7	4.5	27.9
Jul 12	0.52	17.3	48.6	94.8	18.9	36.2	7.5	2.0	84.2	46.7	4.5	32.0
Aug 12	0.59	20.4	59.6	96.7	14.0	27.8	5.9	1.8	71.0	38.2	3.8	21.1
Sep 12	0.54	16.8	49.7	94.4	18.3	36.7	7.6	2.1	82.2	49.0	4.6	27.9
Oct 12	0.57	14.6	42.9	94.0	22.8	42.9	9.1	2.3	79.2	53.5	5.4	42.2
Nov 12	0.57	18.1	50.8	96.6	17.8	35.8	7.0	2.0	70.6	45.9	4.3	32.0
Dec 12	0.59	18.5	53.1	97.7	16.6	33.2	6.7	2.0	65.9	42.7	4.2	27.9
Jan 13	0.57	17.5	50.1	97.1	18.1	35.8	7.3	2.0	68.2	45.6	4.4	32.0
Feb 13	0.56	18.0	52.7	97.6	16.8	33.4	7.0	2.0	66.2	43.1	4.3	32.0
Mar 13	0.57	18.5	54.8	98.9	15.8	31.1	6.7	1.9	59.4	39.7	4.2	32.0

Table 2 Along channel average yearly grain size parameters

Station	< 4	< 16	< 63	> 63	d50	d75	d25	d5	d95	d84	d16	Modal
I	17.5	49.8	95.9	4.1	18.3	36.9	7.3	2.0	73.2	47.8	4.4	36.8
J	18.0	52.7	97.2	2.8	16.8	32.6	7.0	2.0	67.7	42.0	4.3	32.0
K	18.7	53.5	96.8	3.2	16.4	33.2	6.7	0.9	69.7	43.7	4.1	27.8

1.04 with an average of 0.97 over the study period (Table 4). Bottom sediments from the channel had sigma values of 1.56 ϕ to 1.69 ϕ with an average of 1.63 ϕ (Table 4). Skewness values in the channel over the 12 month period ranged from 0.12 to 0.28, average of 0.20, while kurtosis values ranged from 0.93 to 1.00 with an average of 0.94.

The DIGS distributions for all bottom sediments were also analyzed using the process-based parameterization model of Curran et al. (2004). Floc fraction values from all analyzed bottom samples ranged from 0.10 to 0.81 with an average value of 0.53 (Fig. 6; Tables 1 and 3). When all floc fractions were plotted against elevation, no relationship emerged (i.e., $r^2 = 0.03$, Fig. 6). To discern relationships between floc fraction and elevation, samples were separated by their location either on the flat or channel. Floc fraction values from July 2012 in the tidal channel were not correlated with elevation, while floc fraction values on the flat decreased with increasing elevation (Fig. 7a). When the data from July 2012 were binned in 0.25-m elevation intervals, a significant inverse correlation ($r^2 = 0.7$, $p < 0.001$) emerged between floc

fraction and elevation on the tidal flat (Fig. 7b). No such relation existed in the tidal channel. Floc fractions from the channel in March 2013 had similar values to those in July and were not correlated with elevation. In contrast to July, floc fractions on the flat in March increased with increasing elevation (Fig. 8a). When binned, floc fractions were significantly correlated with elevation on the tidal flat ($r^2 = 0.71$, $p < 0.001$; Fig. 8b). Overall, average floc fractions from the same elevations on the flats changed from summer to winter. At higher elevations (i.e., ~18.6 m), floc fractions were ~40% smaller in summer than they were in winter, while at lower elevations (i.e., ~20.2 m), floc fractions were ~70% larger in summer than they were in winter (Figs. 7 and 8).

Significant wave heights in January 2013 were on average twice as large as they were in June 2013 (Fig. 9). Current velocities remained consistent during the summer and winter with average velocities around 0.12 m s⁻¹ (data not shown). Combined wave-current-shear velocities were on average 50% greater in winter compared with the summer sampling (Fig. 9).

Kingsport Flat Average Grain Size

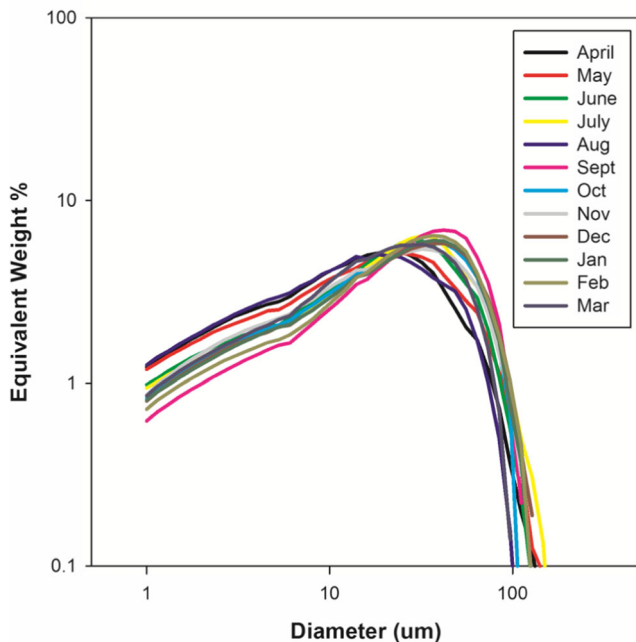


Fig. 5 Average DIGS from the Tidal Flat over the monthly sampling expressed as equivalent weight percent versus diameter in micrometers. In general, coarser DIGS distributions were observed in the summer and fall, and finer DIGS distributions were observed in winter and spring

4 Discussion

Floc fraction, representative of the percentage of fine-grained material deposited in flocs, can be used to understand the formative processes responsible for shaping the bottom sediment texture on the muddy macro-tidal flats at Kingsport. Small changes in floc fraction occurred seasonally in the channel. Values were higher in late winter, and lower in late summer with April having the highest values (Table 1). A more pronounced seasonal variation in floc fraction was observed on the tidal flats, with higher values at higher elevations in late winter and lower values at higher elevations in late summer (Table 3). This pattern is reversed at lower elevations, where higher floc fractions occurred in late summer.

The controls on floc fraction include suspended particulate matter (SPM) concentration, turbulence, and particle stickiness. High SPM concentration promotes higher particle encounter rate and is associated with larger floc fractions (Milligan et al. 2007; Hill et al. 2013). Low-to-moderate turbulence enhances particle encounter rate, which increases floc fraction (Jago et al. 2006), whereas larger turbulence disrupts flocs, which decreases floc fraction (Hill 1996; Milligan and Law 2005). The third control on floc fraction is “stickiness,” and particles with sticky organic coatings are more likely to

Table 3 Yearly average grain size parameters from the tidal flat

Date	FF	< 4	< 16	< 63	d50	d75	d25	d5	d95	d84	d16	Modal
Apr 12	0.74	20.8	58.5	97.3	14.3	28.1	5.9	1.8	67.0	37.1	3.7	24.3
May 12	0.54	19.4	53.7	95.9	16.3	32.6	6.4	1.9	75.0	43.2	3.9	24.3
Jun 12	0.45	16.1	46.6	96.1	19.9	36.2	8.2	2.1	73.3	46.1	4.9	27.9
Jul 12	0.45	15.4	43.9	96.4	21.5	37.9	8.8	2.2	70.7	47.5	5.1	36.8
Aug 12	0.45	21.4	59.8	98.3	13.7	27.7	5.6	1.8	61.6	37.4	3.6	18.4
Sep 12	0.42	11.1	35.1	93.2	27.7	46.8	12.5	2.8	79.9	56.7	7.6	42.2
Oct 12	0.56	14.9	44.0	95.3	21.9	40.7	8.9	2.2	75.3	50.9	5.3	36.8
Nov 12	0.55	16.1	47.1	95.0	19.9	38.7	8.0	2.2	76.9	49.7	4.8	32.0
Dec 12	0.50	14.4	42.1	93.5	23.1	43.1	9.4	2.3	82.0	54.0	5.5	42.2
Jan 13	0.50	14.2	42.0	94.4	23.2	42.4	9.5	2.3	78.4	52.8	5.6	36.8
Feb 13	0.52	12.6	38.5	93.8	25.0	43.7	11.0	2.5	81.1	54.0	6.6	36.8
Mar 13	0.55	15.3	48.3	97.6	19.0	35.1	8.3	2.2	66.3	44.3	5.1	36.8

adhere when they collide. Particles with sticky coatings also are less prone to breakage by turbulence, so they tend to have higher floc fractions.

In a tidally dominated system, flocculation occurs during slack water, when the coincidence of elevated concentration and low-to-moderate turbulence allows flocs to grow (Jago et al. 2006). Flocculation approaching high slack water increases the depositional flux of mud to the seabed by increasing the settling velocity of mud. This process leads to accumulation of muds at higher elevations on tidal flats (e.g., Allen 2000). The sensitivity of flocculation and depositional flux to concentration, turbulence, and stickiness introduces tidal and seasonal variability to grain size on tidal flats. Higher concentrations caused by higher stresses associated with spring tides or larger waves can increase flocculation and decrease grain size on the seabed. Similarly, periods of increased runoff can increase flocculation. Turbulence can counteract the effect of higher concentration, however, by breaking flocs and

decreasing depositional flux of muds, which leads to coarser grain sizes on the bed (e.g., Allen 2000). Seasonal changes in stickiness also affect flocculation and grain size on the seabed.

MERIS satellite imagery to estimate the suspended sediment concentration in the upper Bay of Fundy has shown an order of magnitude increase in suspended sediment concentration in the Minas Basin during the winter months (Tao et al. 2014) (Fig. 10). This order of magnitude concentration difference was validated on two separate cruises to the Minas Basin in summer (i.e., June 2013) and winter 2014 (i.e., March 2014) (Ashall et al. 2016; Zions et al. 2017). Several sources for the winter increase in suspended sediment exist, including greater run off from land, increased erosion from cliffs, ice rafting, and the release of material from tidal flats and creeks as a result of increasing shear stress from wind waves and erosion by raindrops and surface flow (Amos and Long 1980; Amos et al. 1992; Wilson et al. 2017; Hill and Gelati 2017). Changes to the cohesivity of the sediment in response to the loss of bio-films also can lead to greater erosion from tidal flats and channels in winter (Amos and Mosher 1984; Garwood et al. 2015).

Recent work on size sorting during the erosion of cores from the Gulf of Lions, France (Law et al. 2008), and in Seal Harbor, NS (Milligan and Law, 2013), suggests that increases in clay (sediment particles < 4 μm in diameter) changes resuspension dynamics. In sediments that contain > 10% clay, a wide range of sizes are eroded at reduced but equal rates. Sediments with a smaller clay fraction exhibit greater erodibility and size-selective sorting over the entire particle size range. Sediment with a small clay fraction, < 7.5% can be winnowed of its fine fraction during erosion, but sediments with a larger clay fraction cannot. When muddy sands are eroded, the smallest sediment sizes are winnowed from the bed, essentially cleaning the sands. In contrast, when muds are eroded, size sorting is reduced substantially. In short, after deposition, sands are “cleaned” by physical disturbance, but muds resist any further sorting. Even if muds are repeatedly

Table 4 Flat (Fl) and channel (Ch) average monthly folk method of moments data, SD = 1 standard deviation, sk = skewness, and ku = kurtosis

Date	SD Fl	Sk Fl	Ku Fl	SD Ch	Sk Ch	Ku Ch
Apr 12	1.62	0.16	0.94	1.61	0.16	0.94
May 12	1.67	0.18	0.94	1.64	0.16	0.93
Jun 12	1.59	0.26	0.98	1.69	0.19	1.00
Jul 12	1.56	0.30	0.98	1.66	0.22	0.98
Aug 12	1.62	0.15	0.91	1.63	0.12	0.96
Sep 12	1.46	0.33	1.04	1.65	0.18	0.95
Oct 12	1.58	0.27	0.94	1.60	0.28	0.94
Nov 12	1.62	0.23	0.93	1.64	0.21	0.90
Dec 12	1.60	0.27	0.96	1.61	0.20	0.90
Jan 13	1.58	0.29	0.96	1.61	0.23	0.90
Feb 13	1.52	0.30	1.04	1.60	0.20	0.93
Mar 13	1.52	0.24	0.97	1.56	0.21	0.91

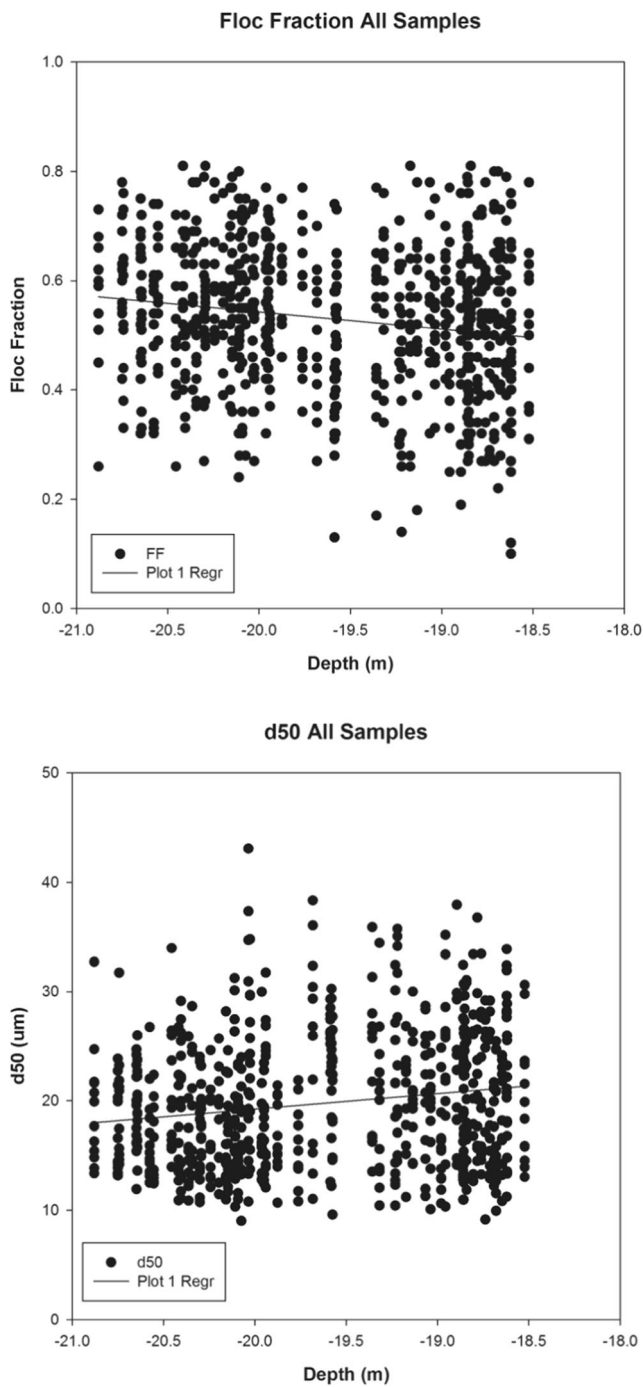


Fig. 6 Floc fraction and d50 for all samples collected from the tidal-channel-flat complex at Kingsport of the monthly sampling ($N=707$). Neither variable is significantly correlated with elevation

resuspended and transported over great distances, they maintain their poorly sorted character and small mean grain size. All samples collected for grain size from the tidal flats and channels at our study site contained $<4\text{-}\mu\text{m}$ fractions greater than 10% and always averaged $>11\%$ and in some months $>20\%$ (Tables 1, 2, and 3). As a result, selective winnowing of the fine fraction from the bed at our location should be limited,

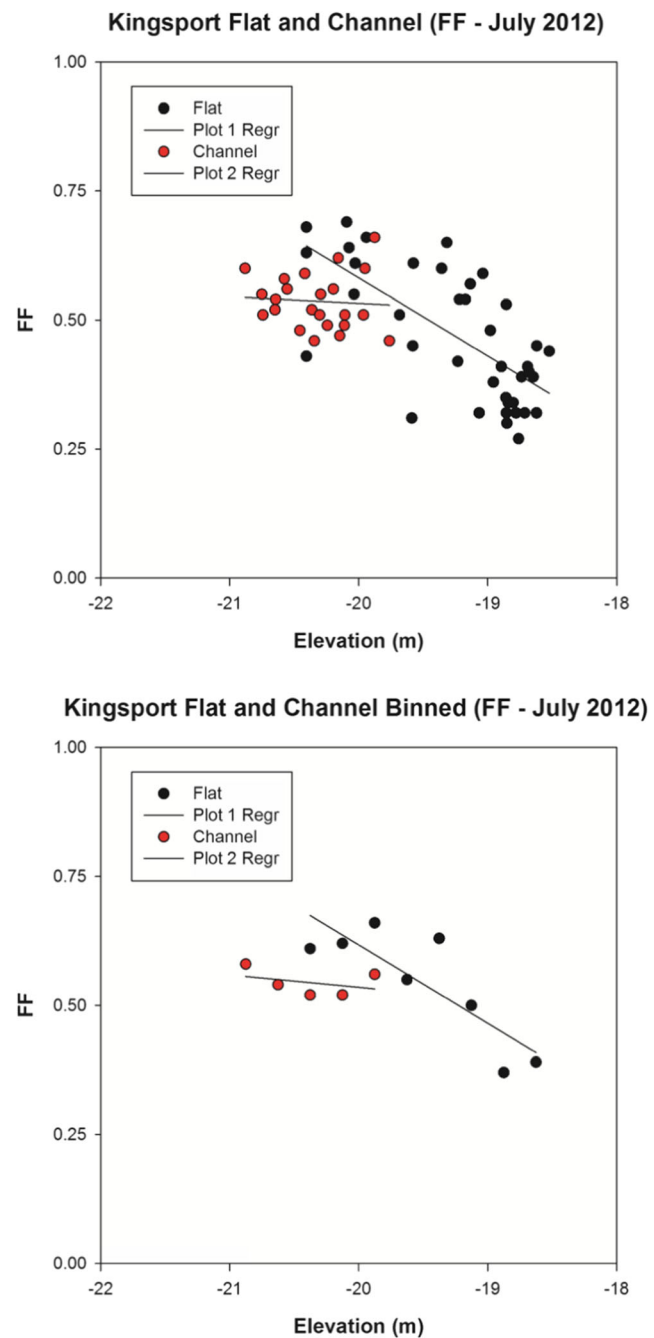


Fig. 7 Floc fraction raw (top) and binned (bottom) from July 2012. Floc fraction from the tidal flat is inversely correlated with elevation, raw ($R^2=0.45$, $p<0.001$), and binned ($R^2=0.70$, $p<0.001$). Channel floc fraction is not correlated with elevation, $R^2=0.01$

so size distributions primarily reflect depositional packaging of sediments.

In macro-tidal areas, turbulence and bottom stress, τ_b , are dominated by tidal flow. Tidal flow in the Inner Bay of Fundy, Minas Basin, does not vary greatly seasonally (Wu et al. 2011; Zions et al. 2017). Wind waves increase during the winter months and subsequently increase turbulence. Deep, sheltered tidal channels remain unaffected by waves during the winter,

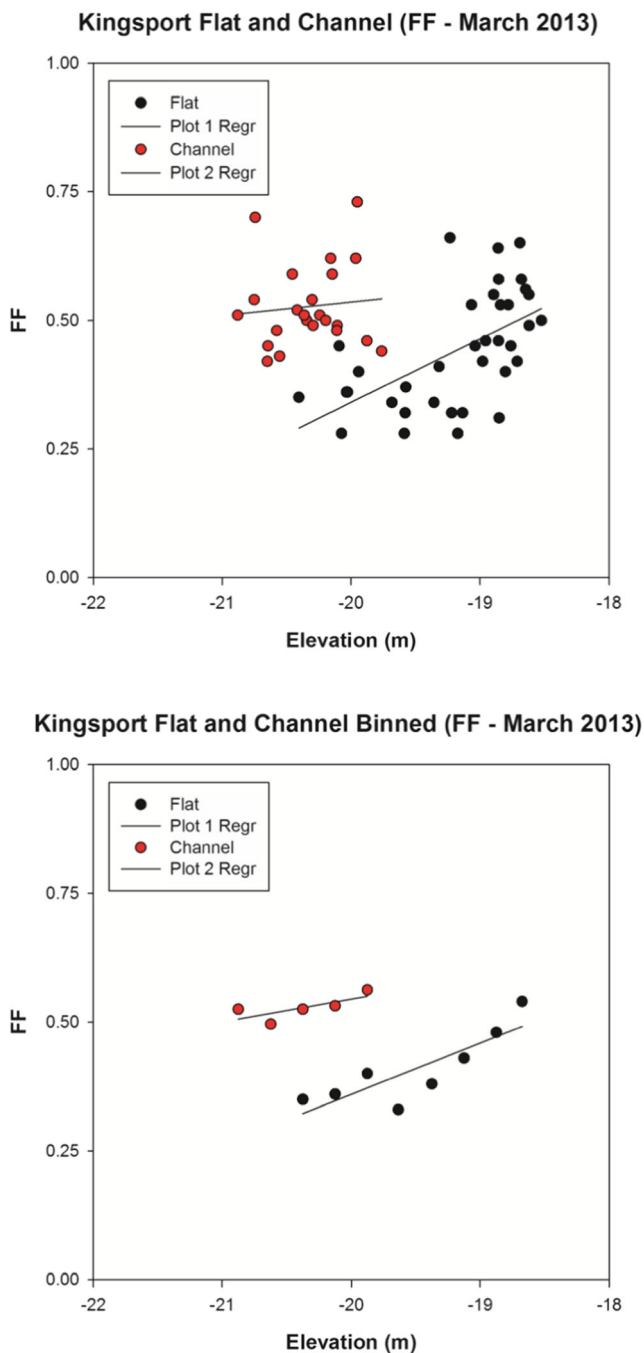


Fig. 8 Floc fraction raw (top) and binned (bottom) from March 2013. Floc fraction from the tidal flat is inversely correlated with elevation, raw ($R^2 = 0.33$, $p < 0.001$), and binned ($R^2 = 0.71$, $p < 0.001$). Channel floc fraction is not correlated with elevation, $R^2 = 0.01$

but more exposed tidal flats experience increases in bottom stress as a direct result of increased wave activity acting upon them (Fig. 9). Although no systematic observations of stickiness were made during this study, observations made by Garwood et al. (2015) in bottom sediments from the study area showed maximum carbohydrate concentrations in spring and minimum in summer. Particles therefore may be stickier

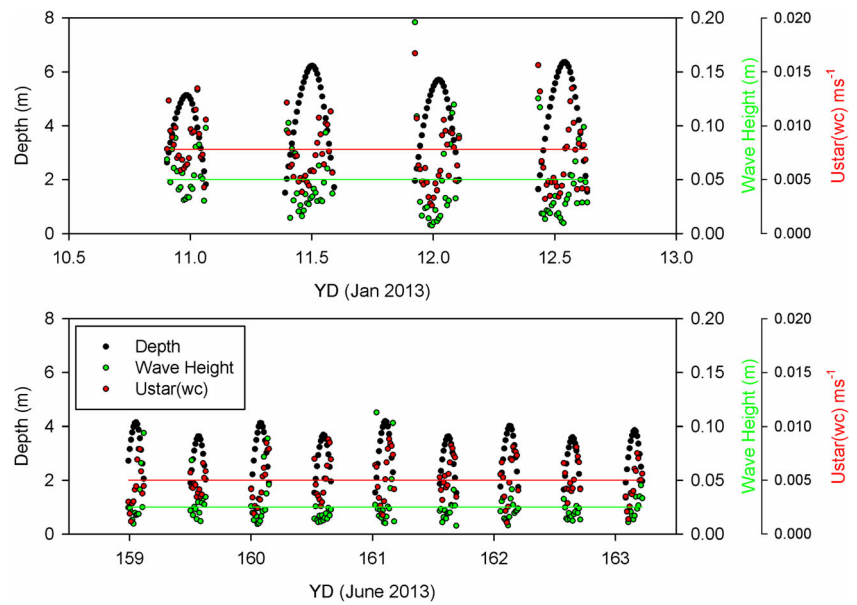
in the spring and less sticky in the summer at times similar to maximum and minimum sediment concentration.

Overall, at Kingsport, there was a trend of higher floc fractions on the tidal flats in winter than in summer. On the tidal flats, low concentration in the summer reduces floc fraction, whereas high concentration in the winter increases floc fraction. Lower suspended-sediment concentrations appear to have a bigger effect on floc fraction than lower turbulence due to less wave activity, and therefore, floc fractions remain low in summer. A similar effect of concentration versus turbulence was observed in winter when high concentration of sediment dominated over the increased shear stress from waves and floc fractions remained high. Low stickiness may also have helped to reduce floc fractions in the summer. In the tidal channel, the lack of variability in floc fraction, with the exception of April, is puzzling because concentration varies seasonally, but seabed stress does not, which suggests that floc fraction should vary with changes in concentration. These results are similar to those found in other studies in the inner Bay of Fundy (O’Laughlin et al. 2014; Poirier et al. 2017). We hypothesize that post-depositional reworking in tidal channels may determine floc fraction instead of depositional packaging. In the channels, sediment may be packaged in toughened “aggregates” that are not disrupted by turbulence.

In this study, no correlation between floc fraction and elevation data existed throughout the monthly sampling in the tidal channels (Figs 7 and 8). O’Laughlin et al. (2014) and Poirier et al. (2017) showed similar dynamics of flocculation albeit on shorter temporal scales. They hypothesized that consistency in floc dynamics was due to the same source of material being present in tidal channels despite changing suspended sediment concentrations and tidal conditions. It was apparent in this study that floc dynamics also remained relatively consistent in the channel as seen in measured floc fraction values over the course of the monthly sampling (Table 1; Figs. 7 and 8).

A distinct relationship emerged between floc fraction and elevation during the summer and the winter on the tidal flats (Figs. 7 and 8). During July 2012, bottom sediments sampled higher up onto the flat (e.g., elevation = -18.63 m) contained the lowest floc fraction values (e.g., $FF = 0.39$), while samples collected at lower elevations (e.g., elevation = -20.38 m) had the highest floc fraction values (e.g., $FF = 0.61$) (Fig. 7). In contrast, samples analyzed from March 2013 from the lowest elevations on the tidal flat (e.g., elevation = -20.38 m) had the lowest floc fraction values (e.g., $FF = 0.35$) and those at the highest elevations (e.g., elevation = -18.68 m) sampled on the tidal flat contain the highest floc fraction values (e.g., $FF = 0.54$) (Fig. 8). The trend of higher floc fraction values for bottom sediments from the tidal flats collected at the lowest elevations observed in July also held for August and September, and the trend observed in March 2013 held in January, February, and April. The correlation between floc

Fig. 9 Plot of water depth (black dots), significant wave heights (green dots), and combined wave-current shear velocity (red dots) for two tidal cycles in Jan 2013 and for 4.5 tidal cycles in June 2013 from our Kingsport sampling site in the middle of our tidal flat. The red and green lines in each plot represent the average wave height and average combined wave current shear velocity for each sampling date



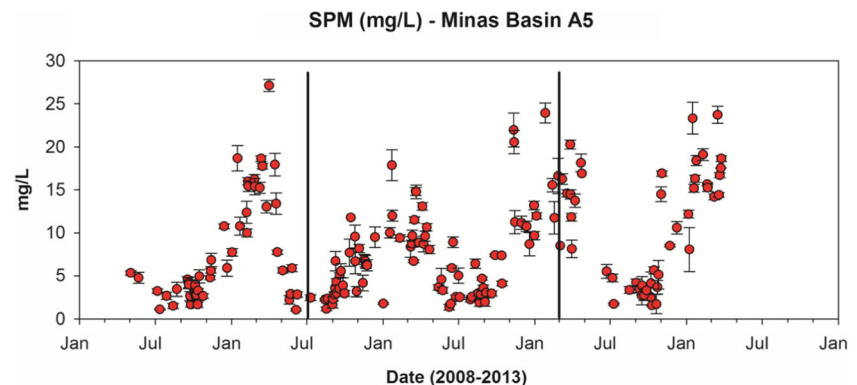
fraction and elevation in other months was weaker ($r^2 < 0.2$), suggesting that October–December and May–June were transitional periods. These seasonal shifts in the spatial distribution of floc fraction contrast with a study by Law et al. (2013) in Willapa Bay on a muddy mesotidal flat in which floc fraction was always inversely correlated with elevation, despite the season. In that study, the finest grain size material was deposited in the form of flocs in the tidal channels and on channel banks which had the lowest elevations.

Changes in SPM at the Kingsport study site overall favor higher floc fractions on the flats in the winter when SPM was larger. The observed decrease in floc fraction at lower elevations on the flats in winter, therefore, must have arisen either from increased turbulence and/or bed shear stresses or decreased particle stickiness. On the assumption that particle stickiness would change similarly across the flats in response to seasonal changes, we propose that changes in turbulence and bed shear stress were responsible for the winter decrease in floc fraction at lower elevations on the flats. The Aquadopp current meter showed increased wave heights and associated

wave-induced shear stresses in the winter versus the summer (Fig. 9). Although the data set only sampled two complete tidal cycles in January 2013, approaching spring tides and four tidal cycles in June 2013, approaching neap tides, both wave heights and combined wave-current stress were higher during the winter sampling even when accounting for water depth (Fig. 9). In addition, winds from the nearby but not on-site, Debert, N.S. airfield (not shown) were $< 7 \text{ m s}^{-1}$ and from a northerly direction during the winter Aquadopp measurements which kept wave heights low. This seasonal change in wave climate likely caused the winter reduction in floc fractions at lower elevations on the flats.

Fagherazzi et al. (2006) demonstrated that a peak in wave stress on tidal flats occurs at a depth that is determined by the wavelength and period of incident waves. At deeper depths, stresses are reduced due to the greater water depth, and at shallower depths, stresses are reduced because of wave attenuation in shallow water and wave breaking. The elevation of maximum stress changes with the season. We propose that higher, longer period waves in winter increased the depth of

Fig. 10 MERIS satellite-derived suspended particulate matter (SPM) concentration from the period of 2008–2013 from the southern bight of Minas Basin. Data courtesy of Ocean Color Group at Bedford Institute of Oceanography



maximum stress. The depths at which flocs deposited at lower wave stresses in summer were exposed to stresses that did not allow flocs to deposit in winter, so floc fraction decreased. The material that failed to deposit lower on the flats in winter was driven higher onto the flats. Higher concentrations over higher elevations on the flats led to increased floc fractions in those areas. The retention of flocs at lower elevations in summer led to higher floc fractions, but the depositional loss of flocs at lower elevations starved the upper flats of sediment, which led to lower floc fractions.

Boldt et al. (2013) and Nowacki and Ogston (2013) observed an order of magnitude difference in suspended sediment concentration in Willapa Bay similar to that observed in our study area, yet floc fractions in Willapa Bay showed no seasonal change with elevation. Boldt et al. (2013) showed that combined wave-current shear stress remained similar throughout the year in Willapa Bay. The summer trend of decreasing floc fraction with increasing elevation at Kingsport was similar to the trend observed in Willapa Bay over the entire year. These contrasting results demonstrate that waves have a depth-localized seasonal role in determining seabed grain size. In environments like Kingsport that experience seasonal changes in wave climate, shifts in grain size as a function of elevation occur. In environments with relatively constant stresses throughout the year, seasonal shifts are absent.

5 Conclusion

Seasonal changes in the trend of floc fraction with elevation on a macro-tidal mud flat are linked to seasonal changes in wave climate. In summer when waves were small, flocs were able to deposit at lower elevations on the tidal flat, which increased floc fraction in surficial sediments. Depositional losses of flocs lower on the flats reduced the concentration of sediment in suspension as water flowed higher onto the flat, which led to a decrease in floc fraction in surficial sediments. In winter when waves were larger, flocs either were smaller or less abundant due to elevated stresses, or they were unable to deposit at lower elevations. These processes caused a decrease in floc fraction at lower elevations. Sediment that did not deposit at lower elevations was pushed higher onto the flats, causing higher floc fractions there.

The observed seasonal change in the trend of floc fraction with elevation was not observed in a similar study on tidal flats in Willapa Bay, which is a mesotidal system in which higher floc fractions persist at lower elevations throughout the year. We attribute the different behaviors to differing seasonal changes in wave energy. At Kingsport, despite a relatively sheltered location, we hypothesize that larger waves occurred during winter, leading to elevation-dependent increases in shear stress and decreases in floc fraction. At Willapa Bay,

we hypothesize that because the orientation of the tidal flats shielded them from winter waves generated by strong southerly winds, wave stresses and floc fractions did not change at lower elevations. These different behaviors indicate that accurate models of sediment size distribution in the seabed in tidally dominated systems need to incorporate wave stresses.

Acknowledgements We would like to thank Casey O’Laughlin, Emma Poirier, Danika vanProosdij, Gary Bugden, Logan Ashall, and Ryan Mulligan for their support in the field and great talks about tidal flats at the Old Port Pub near our study site.

References

- Allen JRL (2000) Morphodynamics of Holocene salt marshes: a review sketch from the Atlantic and Southern North Sea coasts of Europe. *Quat Sci Rev* 19:1155–1231
- Amos CL and Long BFN, 1980. The sedimentary character of Minas Basin, Bay of Fundy. In S.B. McCann (editor). *The coastline of Canada*, Geol Surv Can Pap, 123–152
- Amos CL, Mosher DC (1984) Erosion and deposition of fine-grained sediments from the Bay of Fundy. *Sedimentology* 32:815–832
- Amos CL, VanWagoner NA, Daborn GR (1988) The influence of sub-aerial exposure on the bulk properties of fine-grained intertidal sediment from Minas Basin, Bay of Fundy. *Estuar Coast Shelf Sci* 27: 1–13
- Amos C, Daborn G, Christian H, Atkinson A, Robertson A (1992) In situ erosion measurements on fine-grained sediments from the Bay of Fundy. *Mar Geol* 108:175–196
- Ashall L, Mulligan RP, Law BA (2016) Variability in suspended sediment concentrations in the Minas Basin, Bay of Fundy, and implications of change due to tidal power extraction. *Coast Eng* 107:102–115. <https://doi.org/10.1016/j.coastaleng.2015.10>
- Austen I, Andersen TJ, Edolvang K (1999) The influence of benthic diatoms and invertebrates on the erodibility of an intertidal mudflat, the Danish Wadden Sea. *Estuar Coast Shelf Sci* 49:99–111
- Black KS, Tolhurst TJ, Paterson DM, Hagerthey SE (2002) Working with natural cohesive sediments. *J Hydraul Eng-ASC* 128:2–8
- Boldt KV, Nittrouer CA, Ogston AS, (2013). Seasonal transfer and net accumulation of fine sediment on an Muddy Tidal Flat: Willapa Bay, Washington. *Cont Shelf Res*
- Christiansen T, Wiberg PL, Milligan TG (2000) Flow and sediment transport on a tidal salt marsh surface. *Estuar Coast Shelf Sci* 50:315–331
- Curran KJ, Hill PS, Milligan TG (2002) Fine-grained suspended sediment dynamics in the eel river flood plume. *Cont Shelf Res* 22: 2537–2550
- Curran KJ, Hill PS, Schell TM, Milligan TG, Piper DJW (2004) Inferring the mass fraction of floc-deposited mud: application to fine-grained turbidites. *Sedimentology* 51:927–944
- Daborn, G.R. 1991. LISP 89 Littoral investigation of sediment properties final report
- Dyer KR, Christie MC, Wright EW (2000) The classification of intertidal mudflats. *Cont Shelf Res* 20:1039–1060
- Eisma D (1998) *Intertidal deposits: river mouths, tidal flats, and coastal lagoons*. CRC Press, Boca Raton, Florida, p 525
- Faas R, Christian H, Daborn G and Brylinsky M. 1993. Biological-control of mass properties of surficial sediments—an example from Starrs Point Tidal Flat, Minas Basin, Bay of Fundy
- Fagherazzi S, Carniello C, D’Alpaos L, Defina A (2006) Critical bifurcation of shallow microtidal landforms in tidal flats and salt marshes. *PNAS* 103(22):8337–8341

- Folk RL, 1968, Petrology of sedimentary rocks: Austin, University of Texas Publication, p. 170
- Folk RL, Ward WC (1957) Brazos River bar: a study in the significance of grain size parameters. *J Sediment Petrol* 27:3–26
- Fox JM, Hill PS, Milligan TG, Boldrin A (2004) Flocculation and sedimentation on the Po River Delta. *Mar Geol* 203:95–107
- Garwood JC, Hill PS, MacIntyre HL, Law BA (2015) Grain sizes retained by diatom biofilms during erosion on tidal flats linked to bed sediment texture. *Cont Shelf Res* 104:37–44. <https://doi.org/10.1016/j.csr.2015.05.004>
- George DA, Hill PS, Milligan TG (2007) Flocculation, heavy metals (Cu, Pb, Zn) and the sand-mud transition on the Apennine Margin, Italy. *Cont Shelf Res* 27:475–488
- Gordon DC, Desplanches C (1983) Dynamics and environmental effect in the Cumberland Basin of the Bay of Fundy. *Can J Fish Aquat Sci* 40:1331–1342
- Grant, WD, Madsen OS (1986) The continental shelf bottom boundary layer. *Annual Review of Fluid Mechanics* 18: 265–305
- Harris MM, Avera WE, Abelev A, Bentrem FW, Bibee LD, Mts I (2008) Sensing shallow seafloor and sediment properties, recent history. *Oceans 1–4(2008)*:146–156
- Hill PS (1996) Sectional and discrete representation of floc breakage in agitated suspensions. *Deep-Sea Res I* 43:679–702
- Hill PS, Gelati S (2017) Competent versus observed grain size on the seabed of the Gulf of Maine and Bay of Fundy. *J Coast Res* 33(6): 1261–1270
- Hill PS, Voulgaris G, Trowbridge JH (2001) Controls on floc size in a continental shelf bottom boundary layer. *J Geophys Res* 106:9543–9549
- Hill PS, Newgard J, Law BA, Milligan TG (2013) Flocculation on a muddy intertidal flat in Willapa Bay, Washington, Part II: observations of suspended particle size in a secondary channel and adjacent flat. *Cont Shelf Res* 60(S):S145–S156
- Holland KT, Elmore PA (2008) A review of heterogeneous sediments in coastal environments. *Earth Sci Rev* 89:116–134
- Jago CF, Jones SE, Sykes P, Rippeth T (2006) Temporal variation of suspended particulate matter and turbulence in a high energy, tide-stirred, coastal sea: relative contributions of resuspension and disaggregation. *Cont Shelf Res* 26:2019–2028
- Kirwan ML et al (2010) Limits on the adaptability of coastal marshes to rising sea level. *Geophys Res Lett* 37:L23401
- Knight RJ, Dalrymple RW (1976) Winter conditions in a macro-tidal environment, Cobequid Bay, Nova Scotia. *Rev Géogr Montréal* 30:65–85
- Kranck K (1973) Flocculation of suspended sediment in the sea. *Nature* 246:348–350
- Kranck K (1975) Sediment deposition from flocculated suspensions. *Sedimentology* 22:111–123
- Kranck K (1980) Experiments on the significance of flocculation in the settling of fine-grained sediment in still water. *Can J Earth Sci* 17: 1517–1526
- Kranck, K., Milligan, T.G., 1979. The use of coulter counters in studies of particle size
- Kranck K, Milligan TG (1985) Origin of grain size spectra of suspension deposited sediment. *Geo-Mar Lett* 5:61–66
- Kranck K, Milligan TG (1991) Grain size in oceanography. In: Syvitski JPM (ed) *Principles, Methods and Application of Particle Size Analysis*. Cambridge University Press, New York, pp 322–345
- Kranck K, Smith PC, Milligan TG (1996a) Grain-size characteristics of fine-grained unflocculated sediments I: ‘one-round’ distributions. *Sedimentology* 43:589–596
- Kranck K, Smith PC, Milligan TG (1996b) Grain-size characteristics of fine-grained unflocculated sediment II: ‘multi-round’ distributions. *Sedimentology* 43:597–606
- Law BA, Hill PS, Milligan TG, Curran KJ, Wiberg PL, Wheatcroft RA (2008) Size sorting of fine-grained sediments during erosion: results from the western Gulf of Lions. *Cont Shelf Res* 28:1935–1946
- Law BA, Milligan TG, Hill PS, Newgard N, Wheatcroft RA, Wiberg PL (2013) Flocculation on a muddy intertidal flat in Willapa Bay, Washington, part I: a regional survey of the grain size of surficial sediments. *Cont Shelf Res* 60(S):S136–S144
- Le Hir P, Roberts W, Cazaillet O, Christie M, Bassoullet P, Bacher C (2000) Characterization of intertidal flat hydrodynamics. *Cont Shelf Res* 20:1433–1459
- van Ledden M, van Kesteren WGM, Winterwerp JC (2004) A conceptual framework for the erosion behaviour of sand-mud mixtures. *Cont Shelf Res* 24:1–11
- Madsen OS (1994) Spectral wave-current bottom boundary layer flows. In: *Coastal Engineering 1994*. Proceedings of the 24th International Conference on Coastal Engineering Research Council, Kobe, Japan, pp. 384–398
- McCave IN (1984) Size spectra and aggregation of suspended particles in the deep ocean. *Deep-Sea Res* 31:329–352
- McCave IN, Manighetti B, Robinson SG (1995) Sortable silt and fine sediment size/composition slicing: parameters for palaeocurrent speed and palaeoceanography. *Paleoceanography* 10(3):593–610
- Milligan TG, Kranck K (1991) Electroresistance particle size analyzers. In: Syvitski JPM (ed) *Principles, methods, and application of particle size analysis*. Cambridge University Press, New York, pp 109–118
- Milligan TG, Law BA (2005) The effect of marine aquaculture on fine sediment dynamics in coastal inlets. *Handbook Environ Chem* 5(Part M):239–251
- Milligan TG, Loring DH (1997) The effect of flocculation on the size distributions of bottom sediment in coastal inlets: implications for contaminant transport. *Water Air Soil Pollut* 99:33–42
- Milligan TG, Hill PS, Law BA (2007) Flocculation and the loss of sediment from the Po River plume. *Cont Shelf Res* 27:309–321
- Milligan TG, Law BA (2013) Contaminants at the sediment-water interface: Implications for Environmental Impact Assessment and Effects Monitoring. *Journal of Environmental Science and Technology*, 47(11): 5828–5834. <https://doi.org/10.1021/es3031352>
- Nowacki DJ, Ogston AS (2013). Water and sediment transport of channel-flat systems in a mesotidal mudflat: Willapa Bay, Washington. *Cont Shelf Res*
- O’Laughlin C, vanProosdij D, Milligan TG (2014) Flocculation and sediment deposition in a hypertidal creek. *Cont Shelf Res* 82:72–84
- Poirier E, van Proosdij D, Milligan TG (2017) The effect of source suspended sediment concentration on the sediment dynamics of a macrotidal creek and salt marsh. *Cont Shelf Res* 148:130–138
- van Proosdij D, Milligan T, Bugden G, Butler K (2009) A tale of two macro tidal estuaries: differential morphodynamic response of the intertidal zone to causeway construction. *J Coast Res* 56:772–776
- Reed DJ, Spencer T, Murray AL, French JR, Leonard L (1999) Marsh surface sediment deposition and the role of tidal creeks: Implications for created and managed coastal marshes. *J Coast Conserv* 5:81–90
- Rose EPF, Willig D (2004) Specialist maps prepared by German military geologists for operation sealion: the invasion of England scheduled for September 1940. *Cartogr J* 41(1):13–35
- Santschi PH, Lenhart JJ, Honeyman BD (1997) Heterogeneous processes affecting trace contaminant distribution in estuaries: the role of natural organic matter. *Mar Chem* 58:99–125
- Shields A (1936) Application of the theory of similarity and turbulence research to bedload movement. *Mitt. Preuss. Versuchsamt Wasserbau Schiffbau* 26:5–24
- Soulsby R (1997) Dynamics of marine sands. In: *A manual for practical applications*. Thomas Telford Publ, London
- Sternberg RW, Berhane I, Ogston AS (1999) Measurement of size and settling velocity of suspended aggregates on the Northern California continental shelf. *Mar Geol* 154:43–54

- Tao J, Hill PS, Mulligan RP, Smith PC (2014) Seasonal variability of total suspended matter in Minas Basin, Bay of Fundy. *Estuar Coast Shelf Sci* 151:169–180
- Townend I, Whitehead P (2003) A preliminary net sediment budget for the Humber estuary. *Sci Total Environ* 314:755–767
- Wiberg PL, Smith DJ (1987) Calculations of the critical shear stress for motion of uniform and heterogeneous sediments. *Water Resour Res* 23:1471–1478
- Wiberg PL, Drake DE, Cacchione DA (1994) Sediment resuspension and bed armoring during high bottom stress events on the northern California inner continental shelf: measurements and predictions. *Cont Shelf Res* 14(10–11):1191–1219
- Widdows J, Brinsley M (2002) Impact of biotic and abiotic processes on sediment dynamics and the consequences to the structure and functioning of the intertidal zone. *J Sea Res* 48:143–156
- Wilson EK, Hill PS, vanProosdij D, Ruhl M (2017) Coastal retreat rates and sediment input into the Minas Basin, Nova Scotia. *Can J Earth Sci* 54(4):370–378
- Wu Y, Chaffey J, Greenberg DA, Colbo K, Smith PC (2011) Tidally-induced sediment transport patterns in the upper Bay of Fundy: a numerical study. *Cont Shelf Res* 31(19):2041–2053
- Ysebaert T, Herman PMJ (2002) Spatial and temporal variation in benthic macrofauna and relationships with environmental variables in an estuarine, intertidal soft-sediment environment. *Marine Ecology-Progress Series* 244:105–124
- Zions VS, Law BA, O’Laughlin C, Morrison KJ, Drozdowski A, Bugden GL, Home E, Roach S (2017) Spatial and temporal characteristics of water column and seabed sediment samples from Minas Basin, Bay of Fundy. *Can Tech Rep Fish Aquat Sci* 3233:vi–95
- Zwolsman JJG, van Eck GTM, Burger G (1996) Spatial and temporal distribution of trace metals in sediments from the Scheldt Estuary, South-West Netherlands. *Estuar Coast Shelf Sci* 43:55–79